







A Defected Ground Structure Based on Matryoshka Geometry

Alfredo Gomes Neto , Jefferson Costa e Silva , Ianes Barbosa Grécia Coutinho ,
Saulo Souto Camilo Filho , Danila Araújo Santos , Bruno Lima Cavalcanti de Albuquerque 
Group of Telecommunications and Applied Electromagnetism, GTEMA
Federal Institute of Paraíba, IFPB, Brazil
alfredogomes@ifpb.edu.br, jefferson@ifpb.edu.br, ianesgrecia@gmail.com,
saulo.camilo@academico.ifpb.edu.br, danila.araujo@academico.ifpb.edu.br,
bruno.albuquerque@academico.ifpb.edu.br

Abstract—A Defected Ground Structure, DGS, based on matryoshka geometry is described in this paper. The proposed DGS geometry is outlined and initial design equations are presented. Four prototypes, with resonant frequencies 2.17 GHz, 2.44 GHz, 2.99 GHz and 3.73 GHz, were designed, fabricated and characterized, observing a good agreement between measured and numerical results. Also, the obtained results demonstrated the initial design equations usefulness. The resonant behavior was analyzed in terms of the current density and it is possible to observe the current density blocked at the resonant frequency. When compared with dumbbell DGS, a reduction in the resonant frequency up to 47.19% is achieved, confirming the matryoshka geometry miniaturization properties. Furthermore, still comparing with dumbbell geometry, DGS based on matryoshka geometry are more selective.

Index Terms— Band-stop, DGS, filter, matryoshka geometry, miniaturization.

I. INTRODUCTION

Defected ground structures, DGS, are versatile structures and since their first appearances [1]-[3], DGS have found several applications such as filters [4], [5], power dividers [6], [7], antennas [8], [9], sensors [10], [11] and wireless power transfer [12], [13]. Basically, the DGS is formed by modifying the ground plane of a planar transmission line (e.g., microstrip, coplanar and conductor backed coplanar wave guide) removing a small selected geometry from the ground metal, Fig. 1. This modification disturbs the shield current distribution in the ground plane, changing characteristics of the planar transmission line such as line capacitance and inductance [3].

The removed geometry is one of the most flexible parameters in the DGS design, whereby adjustments can be made to achieve a desired frequency response. Despite the variety of DGS geometries (dumbbell, spiral head, arrowhead-slot, “H”, shape slots, a square open-loop with a slot in middle section, open-loop dumbbell, interdigital etc.) [2], [3], the continuous evolution of telecommunication systems, with specific frequency response requirements, as well as recent applications, such as sensors and wireless power transfer, impose an ongoing challenge for microwave

and RF engineers, demanding new geometries to meet these requirements. In this context, a DGS based on the matryoshka geometry is introduced herein.

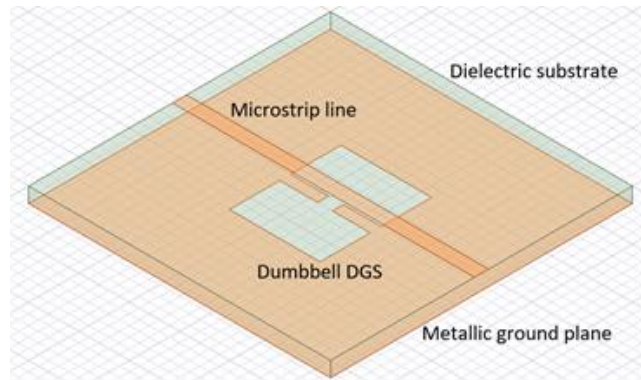


Fig. 1. Example of DGS – Dumbbell geometry.

The matryoshka geometry is characterized by the interconnecting of its concentric rings, increasing its effective length, L_{eff} , without make greater the occupied area, limited to the outmost ring area, Fig. 2, [14]. This characteristic gives the matryoshka geometry interesting properties for RF and microwave applications, such as miniaturization and multiband operation. Frequency selective surfaces, FSS [14], [15], filters [16] and sensors [17] are examples of applications of matryoshka geometry and its variations.

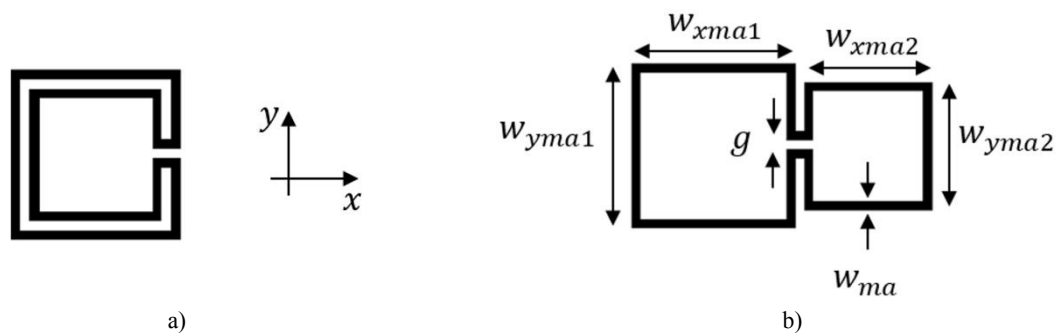


Fig. 2. Matryoshka geometry. a) Matryoshka ring, b) Expanded matryoshka ring.

In this paper a DGS based on matryoshka geometry is introduced, Fig. 3. The main idea is to take advantage of the miniaturization characteristics of matryoshka geometry to obtain DGS with smaller dimensions and more selective, when compared to usual geometries, such as dumbbell. Initial design equations are presented and four prototypes were fabricated and characterized, verifying a good agreement between numerical and experimental results. The results obtained make the proposed DGS potentially attractive for applications in current telecommunications systems and sensors. After this Introduction, the design of the proposed DGS is described in Section II. Numerical and measured results are presented in Section III. In Section IV, conclusions are commented.

II. PROPOSED DGS DESIGN

In this paper the matryoshka ring is centered under the microstrip, as depicted in Fig. 3. The microstrip width is w , the substrate thickness h and its dielectric constant ϵ_r . Although it is possible to use a greater number of rings, as this is a first paper considering DSG based on matryoshka geometry, in this work we choose to use only one matryoshka ring, composed of two interconnected concentric rings. In this case, to obtain the matryoshka geometry, initially two concentric rings are designed, Fig. 4(a). Then, gaps are inserted at the same position in the rings, Fig. 4(b). Finally, the rings are interconnected and the matryoshka ring is achieved, Fig. 4(c). It is worth mentioning here that in the proposed DGS, similarly to band pass FSS [15], this matryoshka geometry is detached from ground plane metallization.

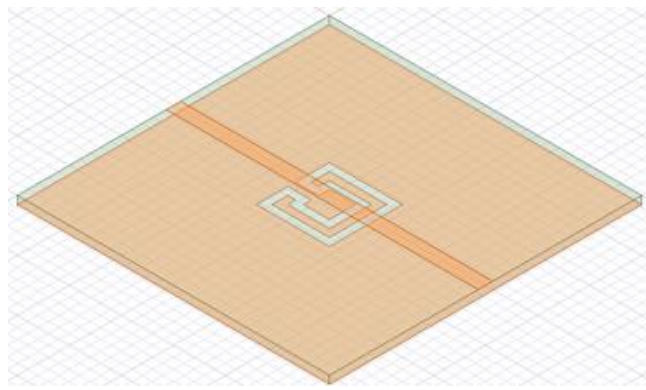


Fig. 3. DGS based on matryoshka geometry.

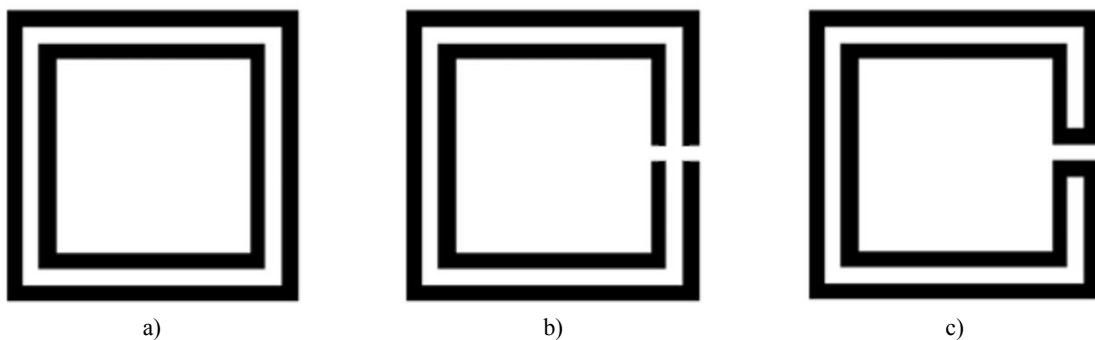


Fig. 4. Matryoshka geometry step by step. a) Concentric rings, b) Gaps at the same position, c) Interconnected rings.

Usually, $w_{xma1} = w_{yma1} = w_{ma1}$ and $w_{xma2} = w_{yma2} = w_{ma2}$. As a first approach, the resonant frequency, $f_{res-calc}$, can be estimated by:

$$f_{res-calc}(GHz) = \frac{0.3}{L_{eff}\sqrt{\epsilon_{reff}}}, \quad (1)$$

with the effective length, L_{eff} , calculated by the following equation:

$$L_{eff} = 3 \times (w_{ma1-avg} + w_{ma2-avg}). \quad (2)$$

and,

$$w_{mai-avg} = w_{mai} - \frac{w_{ma}}{2}, \quad i = 1,2. \quad (3)$$

ϵ_{reff} is the effective dielectric constant for the microstrip line and it can be easily calculated using available software [18].

Note that (1) is similar to the equation for calculating the resonant frequency of a loop-type FSS, for which resonance occurs when the effective length of the loop, herein given by (2), is approximately one wavelength long [19]. Furthermore, despite no optimization was performed in this paper, it must be highlighted that (1)–(3) are initial design equations, and, if necessary, the obtained values can be used as a first approach for a numerical optimization.

III. NUMERICAL AND MEASURED RESULTS

In order to verify the characteristics of the proposed DGS geometry, four DGS were designed, fabricated and characterized. Furthermore, DGS dimensions were chosen in order to obtain resonant frequencies approximately ranging from 2.0 GHz to 3.7 GHz, which included 2.4 GHz and 3.5 GHz bands, widely used in telecommunications systems. Numerical results were obtained using ANSYS HFSS software [21], taking into account the fabricated DGS characteristics. Measured results were acquired at the GTEMA/IFPB microwave measurements laboratory using an Agilent E5071C two ports network analyzer, Fig. 5.

The DGS were fabricated using a low-cost fiber-glass FR-4 substrate ($\epsilon_r = 4.4$, loss tangent $tg(\delta) = 0.02$, thickness $h = 1.6$ mm), with a microstrip width $w = 2.8$ mm. Considering the DGS fabrication technique limits, a gap size of 1 mm was adopted. Table I presents the DGS dimensions. All DGSs were built using the same technique, pasting an adhesive at the ground plane and then the geometry is carried out by chemical attack with ferric chloride. Unfortunately, as consequence of excessive chemical attack exposure, some straight corners were rounded, as can be seen by comparing Figs. 6, 7 and 8 with Fig. 9. However, for this research purposes, it does not significantly affect the DGS frequency response.

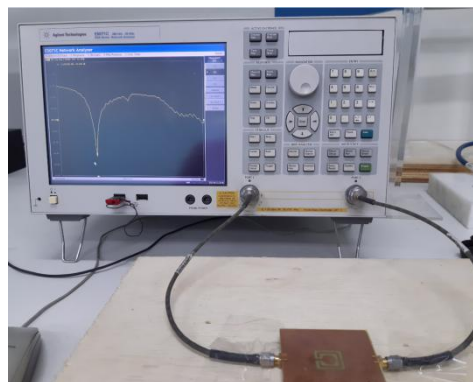


Fig. 5. Measurement setup – DGS bottom view.

TABLE I – FABRICATED DGS DIMENSIONS

	w_{ma1}	w_{ma2}	w_{ma}	g
DGS1	17.0 mm	11.0 mm	1.5 mm	1.0 mm
DGS2	15.5 mm	9.5 mm	1.5 mm	1.0 mm
DGS3	14.0 mm	8.0 mm	1.5 mm	1.0 mm
DGS4	12.5 mm	6.5 mm	1.5 mm	1.0 mm

The frequency responses for DGS1 to DGS4 are presented in Figs. 6 to 9, respectively, verifying a very good agreement between numerical and measured results. As usual DGS, a band-stop frequency response is observed. Table II summarizes the obtained results, where $f_{res-meas.}$ is the measured resonant frequency, and $f_{res-num.}$ is the obtained result from numerical simulation. Furthermore, the resonant frequencies calculated using (1)-(3), $f_{res-calc.}$, when compared to measured results, also present a good approximation, indicating that they are adequate to determine the initial dimensions of DGS based on matryoshka geometry.

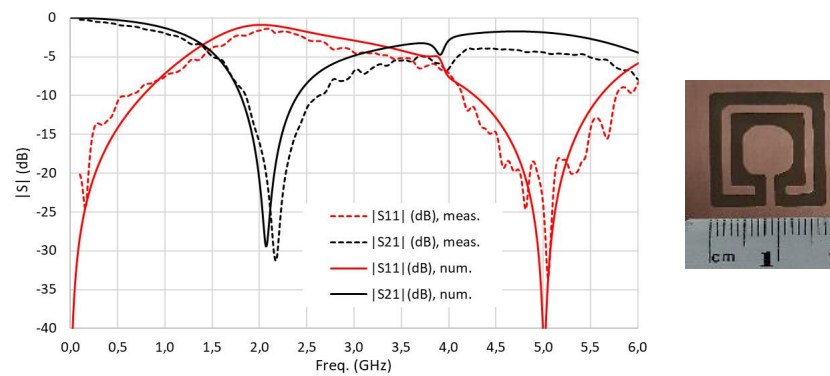


Fig. 6. $|S|(dB) \times Freq.(GHz)$, DGS1, $w_{ma1} = 17.0\text{ mm}$, $w_{ma2} = 11.0\text{ mm}$.

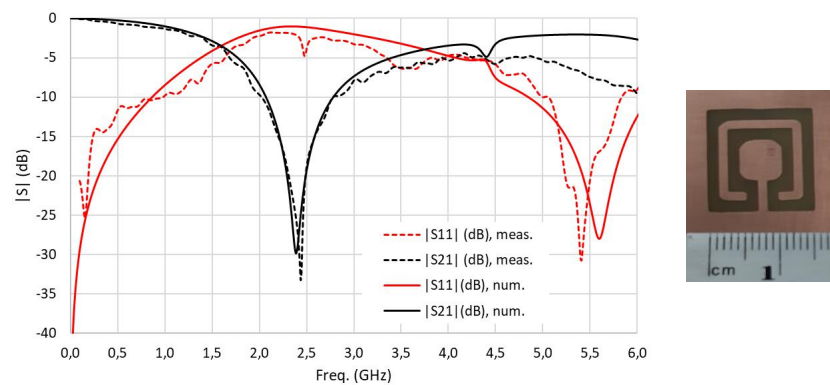


Fig. 7. $|S|(dB) \times Freq.(GHz)$, DGS2, $w_{ma1} = 15.5\text{ mm}$, $w_{ma2} = 9.5\text{ mm}$.

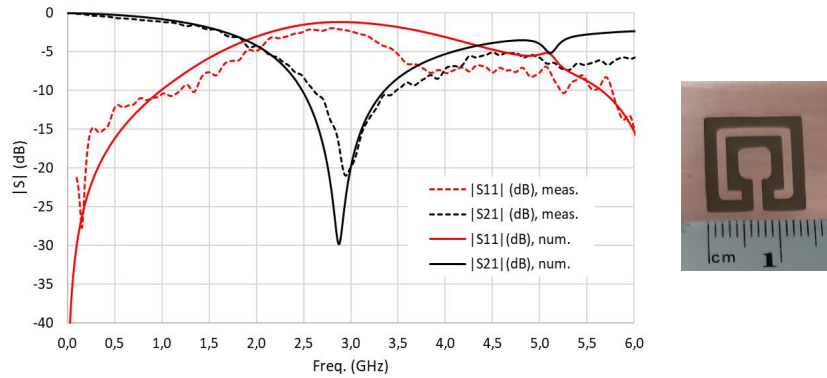


Fig. 8. $|S|(\text{dB}) \times \text{Freq.}(\text{GHz})$, DGS3, $w_{ma1} = 14.0 \text{ mm}$, $w_{ma2} = 8.0 \text{ mm}$.

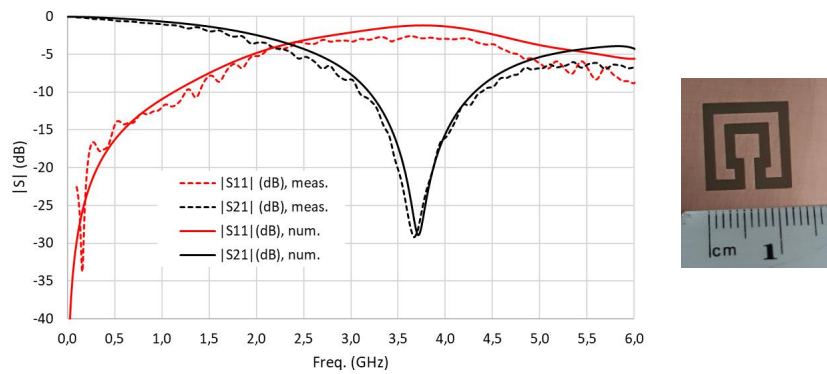


Fig. 9. $|S|(\text{dB}) \times \text{Freq.}(\text{GHz})$, DGS4, $w_{ma1} = 12.5 \text{ mm}$, $w_{ma2} = 6.5 \text{ mm}$.

TABLE II – DGS RESONANT FREQUENCIES

	$f_{res-meas.}$	$f_{res-num.}$	$dif\%_{num./meas.}$	$f_{res-calc.}$	$dif\%_{calc./meas.}$
DGS1	2.17 GHz	2.07 GHz	-4.61 %	2.19 GHz	1.15%
DGS2	2.44 GHz	2.39 GHz	-2.05 %	2.49 GHz	2.22%
DGS3	2.99 GHz	2.88 GHz	-3.68 %	2.89 GHz	-3.41%
DGS4	3.73 GHz	3.72 GHz	-0.27 %	3.43 GHz	-8.05%

Aiming to verify the proposed DGS miniaturization properties, in Figs. 10 to 13, frequency responses are compared for the proposed DGS with dumbbell DGS occupying the same area. For example, dumbbell (17.0 mm) means that the dumbbell DGS has a side width of 17.0 mm. Table III summarizes the obtained results for the resonant frequencies, and it is observed that the proposed DGS resonant frequency is up to 47.19% lower than the equivalent dumbbell DGS (2.07 GHz/3.92 GHz), confirming the miniaturization characteristics of the matryoshka geometry. Furthermore, DGS based on matryoshka geometry are more selective than dumbbell DGS. Considering -10 dB as a reference level, results for the achieved bandwidth and quality factor are presented in Table IV.

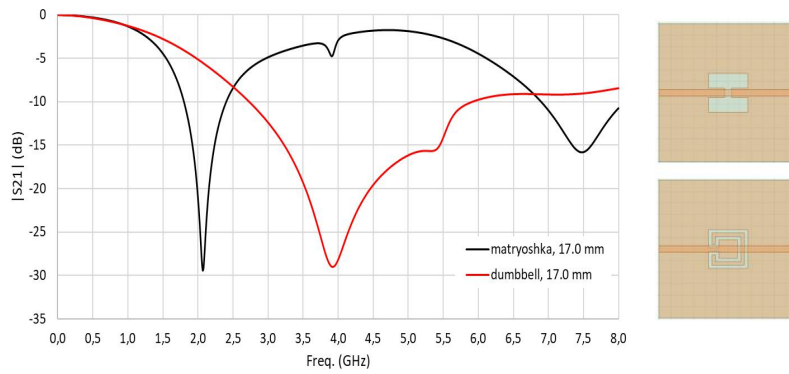


Fig. 10. $|S_{21}|(\text{dB}) \times \text{Freq.}(\text{GHz})$, DGS2 (17.0 mm) and dumbbell (17.0 mm).

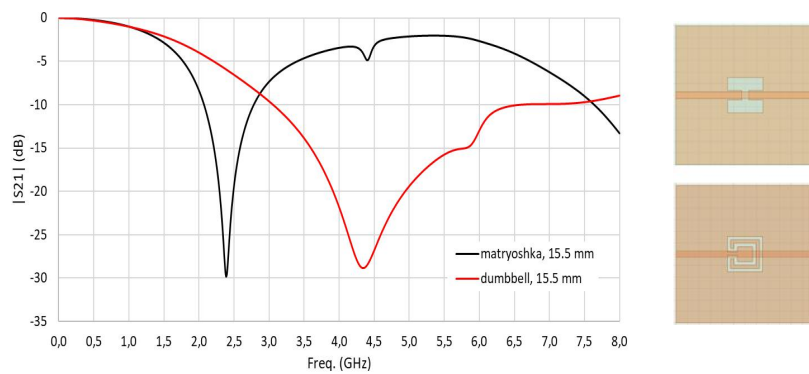


Fig. 11. $|S_{21}|(\text{dB}) \times \text{Freq.}(\text{GHz})$, DGS2 (15.5 mm) and dumbbell (15.5 mm).

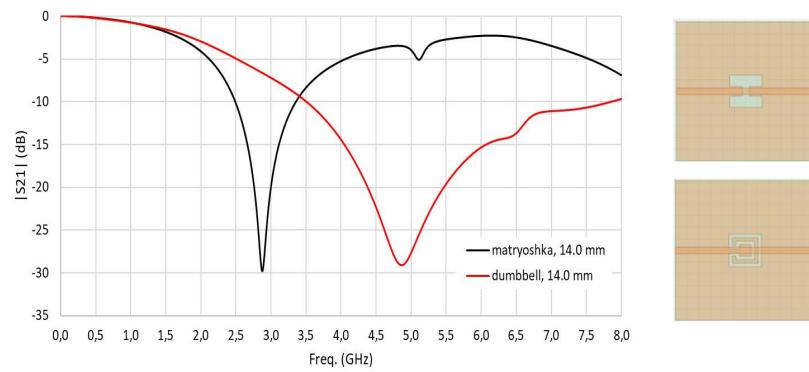


Fig. 12. $|S_{21}|(\text{dB}) \times \text{Freq.}(\text{GHz})$, DGS3 (14.0 mm) and dumbbell (14.0 mm).

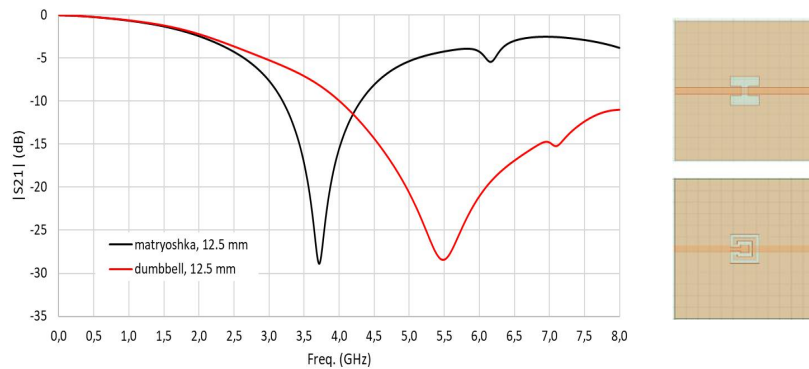


Fig. 13. $|S_{21}|(\text{dB}) \times \text{Freq.}(\text{GHz})$, DGS4 (12.5 mm) and dumbbell (12.5 mm).

TABLE III – DGS RESONANT FREQUENCIES – MATRYOSHKA VERSUS DUMBBELL

	$f_{res-DGS}$		$f_{res-Dumbbell}$	$\left(\frac{f_{res-DGS}}{f_{res-Dumbbell}}\right)\%$
DGS1	2.07 GHz	Dumbbell 17.0 mm	3.92 GHz	52,81%
DGS2	2.39 GHz	Dumbbell 15.5 mm	4.34 GHz	55,07%
DGS3	2.88 GHz	Dumbbell 14.0 mm	4.87 GHz	59,14%
DGS4	3.72 GHz	Dumbbell 12.5 mm	5.48 GHz	67,88%

TABLE IV – DGS BANDWIDTHS AND QUALITY FACTOR – MATRYOSHKA VERSUS DUMBBELL

	$BW_{num.}$	Q		$BW_{num.}$	Q
DGS1	0.59 GHz	3.51	Dumbbell 17.0 mm	3.17 GHz	1.24
DGS2	0.70 GHz	3.41	Dumbbell 15.5 mm	3.54 GHz	1.23
DGS3	0.86 GHz	3.34	Dumbbell 14.0 mm	4.35 GHz	1.12
DGS4	1.10 GHz	3.38	Dumbbell 12.5 mm	> 3.98 GHz	< 1.38

In Figs. 14 to 17, the current density is presented for the DGS1 to DGS4, respectively, considering three frequency points, one of them the resonant frequency. It is possible to observe that at the resonant frequency the current density is blocked.

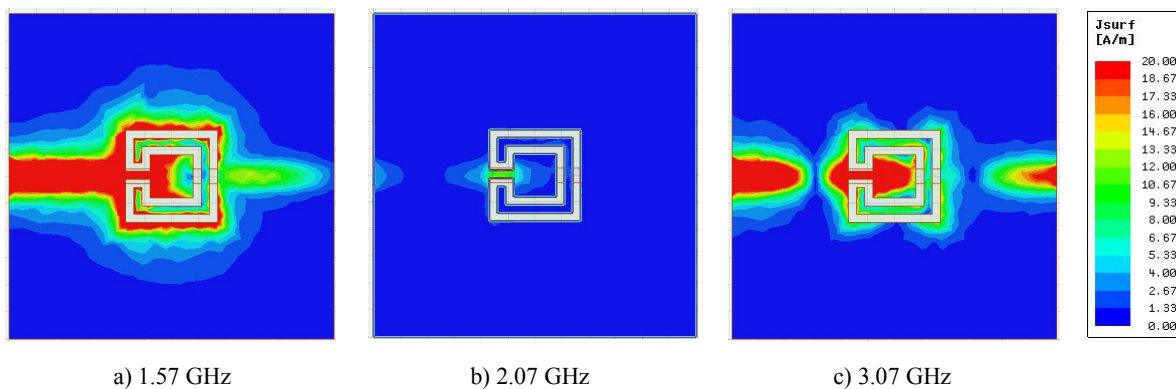


Fig. 14. DGS1 (17.0 mm), bottom view, current density (A/m).

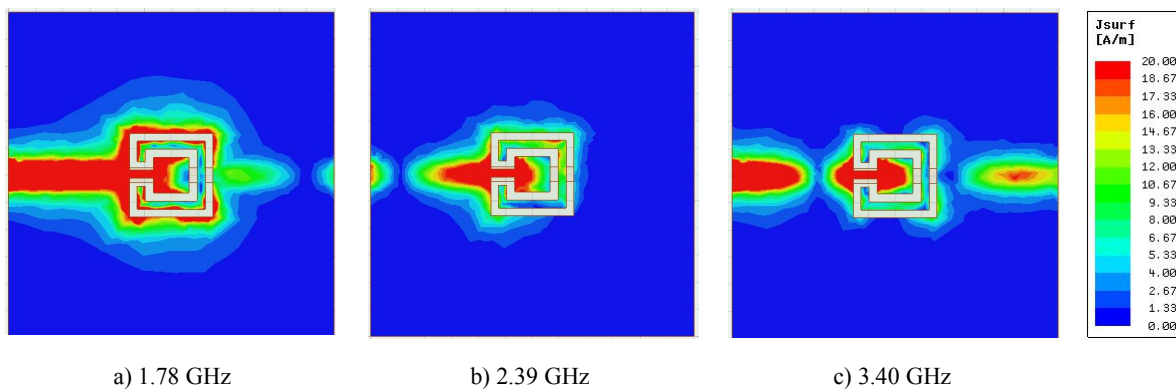


Fig. 15. DGS2 (15.5 mm), bottom view, current density (A/m).

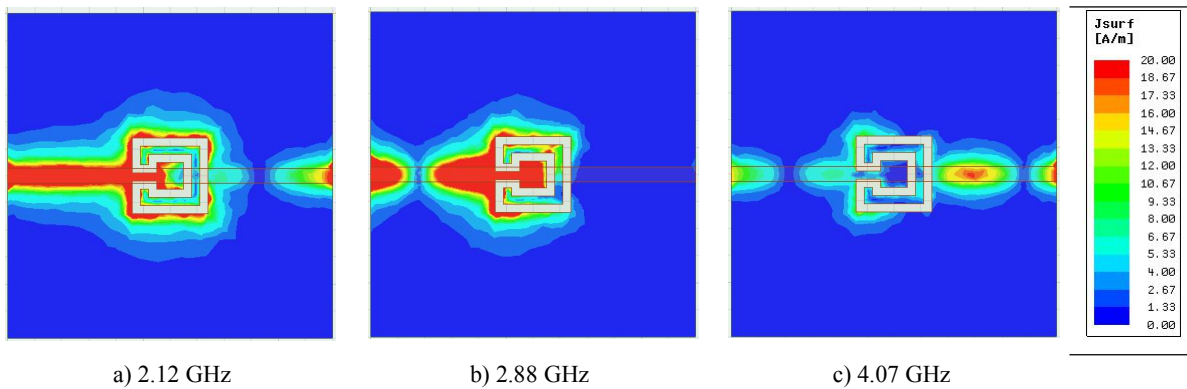


Fig. 16. DGS3 (14.0 mm), bottom view, current density (A/m).

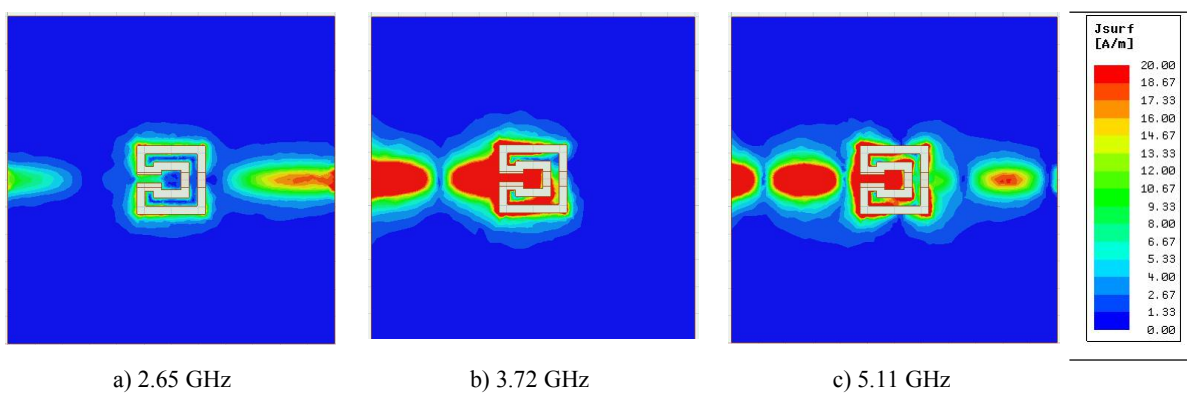


Fig. 17. DGS4 (12.5 mm), bottom view, current density (A/m).

IV. CONCLUSIONS

In this paper, a DGS based on matryoshka geometry was described. This DGS geometry keeps the reduction of the resonant frequency, miniaturization, an interesting feature previously observed in FSS and filter applications. Besides the miniaturization, DGS based on matryoshka geometry are more selective.

Four prototypes were designed, fabricated and characterized. A good agreement between numerical and measured results was verified. Also, the proposed initial design equations gave good results, making easy the design of the DGS for other resonant frequencies and specific applications. An analysis of the resonant behavior in terms of current density is shown, for which it is possible to observe that the current density is blocked at the resonant frequency.

The characteristics observed make the proposed DGS potentially interesting for diverse applications in telecommunication systems, especially in filters design and optimization. However, as this is one of the first paper about the DGS based on matryoshka geometry, many important characteristics still need to be addressed. The geometry design (e.g., gap size, number of rings, and slot width) and its relation to the frequency response parameters (e.g., bandwidth, resonant frequency, and multiresonant behavior) is an instigating subject, that must be explored in future works.

ACKNOWLEDGMENT

This work is supported by the Brazilian National Council of Scientific and Technological Development (Notice 17/2020 - PIBITI/CNPq, Notice 27/2021 - PIBITI/CNPq), and the Federal Institute of Paraíba Postgraduate Program in Electrical Engineering (PPGEE-IFPB).

REFERENCES

- [1] J. Park, C. Kim, J. Kim, J. Park, Y. Qian, D. Ahn, and T. Itoh, "Modeling of a photonic bandgap and its application for the low-pass filter design," *1999 Asia Pacific Microwave Conference, APMC'99*, Singapore, 1999, pp. 331-334 vol.2, doi: 10.1109/APMC.1999.829865.
- [2] M. K. Khandelwal, B. K. Kanaujia, and S. Kumar, "Defected ground structure: fundamentals, analysis, and applications in modern wireless trends," *Hindawi International Journal of Antennas and Propagation*, vol. 2017, pp.1-22, 2017, doi: 10.1155/2017/2018527.
- [3] L. H. Weng, Y. C. Guo, X. W. Shi, and X. Chen, "An Overview on defected ground structure," *Progress in Electromagnetics Research B*, vol. 7, pp. 173-189, 2008. doi:10.2528/PIERB08031401
- [4] J. Zhou, Y. Rao, D. Yang, H. J. Qian and X. Luo, "Compact wideband BPF with wide stopband using substrate integrated defected ground structure," *IEEE Microwave and Wireless Components Letters*, vol. 31, no. 4, pp. 353-356, April 2021, doi: 10.1109/LMWC.2021.3053756.
- [5] S. Cao, Y. Han, H. Chen and J. Li, "An Ultra-Wide Stop-Band LPF Using Asymmetric Pi-Shaped Koch Fractal DGS," *IEEE Access*, vol. 5, pp. 27126-27131, 2017, doi: 10.1109/ACCESS.2017.2773577.
- [6] M. Farooq, A. Abdullah, M. A. Zakir and H. M. Cheema, "Miniaturization of a 3-way power divider using defected ground structures," *2019 IEEE Asia-Pacific Microwave Conference (APMC)*, 2019, pp. 1503-1505, doi: 10.1109/APMC46564.2019.9038858.
- [7] Seongmin Oh, Jae-Jin Koo, Mun-Su Hwang, Chunseon Park, Yong-Chae Jeong, Jong-Sik Lim, Kwan-Sun Choi, and Dal Ahn, "An unequal Wilkinson power divider with variable dividing ratio," *2007 IEEE/MTT-S International Microwave Symposium*, 2007, pp. 411-414, doi: 10.1109/MWSYM.2007.380475.
- [8] S. Pandit, P. Ray and A. Mohan, "Compact MIMO antenna enabled by DGS for WLAN applications," *2018 IEEE International Symposium on Antennas and Propagation & USNC/URSI National Radio Science Meeting*, 2018, pp. 35-36, doi: 10.1109/APUSNCURSINRSM.2018.8609389.
- [9] F. A. A. de Souza, A. L. P. S. Campos, A. Gomes Neto, A. J. R. Serres, and C. C. R. Albuquerque, "Higher order mode attenuation in microstrip patch antenna with DGS H filter specification from 5 to 10 GHz range," *Journal of Microwaves, Optoelectronics and Electromagnetic Applications (JMoe)*, vol. 19, no. 2, pp. 214-227, June 2020, doi.org/10.1590/2179-10742020v19i2823
- [10] E. Mansour, A. Allam and A. B. Abdel-Rahman, "A novel approach to non-invasive blood glucose sensing based on a defected ground structure," *2021 15th European Conference on Antennas and Propagation (EuCAP)*, 2021, pp. 1-5, doi: 10.23919/EuCAP51087.2021.9411425.
- [11] J. G. D. Oliveira, J. G. Duarte Junior, E. N. M. G. Pinto, V. P. Silva Neto, and A. G. D'Assunção, "A new planar microwave sensor for building materials complex permittivity characterization" *Sensors*, vol. 20, no. 21, p. 6328. <https://doi.org/10.3390/s20216328>
- [12] K. Dautov, M. Hashmi, G. Naurzybayev and N. Nasimuddin, "Recent advancements in defected ground structure-based near-field wireless power transfer systems," *IEEE Access*, vol. 8, pp. 81298-81309, 2020, doi: 10.1109/ACCESS.2020.2991269.
- [13] S. Hekal, A. B. Abdel-Rahman, H. Jia, A. Allam, A. Barakat and R. K. Pokharel, "A novel technique for compact size wireless power transfer applications using defected ground structures," *IEEE Transactions on Microwave Theory and Techniques*, vol. 65, no. 2, pp. 591-599, Feb. 2017, doi: 10.1109/TMTT.2016.2618919.
- [14] A. Gomes Neto, J. C. e Silva, J. N. de Carvalho, J. do N. Cruz, H. de P. A. Ferreira, "Analysis of the resonant behavior of FSS using Matryoshka geometry," in *2015 SBMO/IEEE MTT-S International Microwave and Optoelectronics Conference (IMOC)*, Porto de Galinhas, Brazil, Nov. 2015, pp. 1-5.
- [15] A. Gomes Neto, J. C. e Silva, A. J. R. Serres, M. de O. Alencar, I. B. G. Coutinho, T. da S. Evangelista, "Dual-band band-pass frequency selective surface based on the matryoshka geometry with angular stability and polarization independence," *2020 14th European Conference on Antennas and Propagation (EuCAP)*, 2020, pp. 1-4, doi: 10.23919/EuCAP48036.2020.9135542.
- [16] A. Gomes Neto, A. Flor Neto, M.C. Andrade, J. C. e Silva, J. N. de Carvalho, "Filtros em microfitas utilizando a geometria anéis Matryoshka circulares," in *portuguese*, in: *18° SBMO/13° CBMag*, 2018, Santa Rita do Sapucaí, MG. pp. 366-370.
- [17] A. Gomes Neto, A. Gonçalves da Costa and C. da Silva Moreira, T. R. de Sousa, I. B. G. Coutinho "A new planar sensor based on the matryoshka microstrip resonator," *2017 SBMO/IEEE MTT-S International Microwave and Optoelectronics Conference (IMOC)*, 2017, pp. 1-5, doi: 10.1109/IMOC.2017.8121074.
- [18] <http://www.hp.woodshot.com>.
- [19] B. A. Munk, *Frequency Selective Surfaces – Theory and design*, Wiley, New York, 2000.